

Today

Manuscript Draft

Manuscript Number: CATTOD-D-17-00073R1

Title: Ethanol steam reforming on nanostructured catalysts of Ni, Co and CeO<sub>2</sub>: Influence of synthesis method on activity, deactivation and regenerability

Article Type: SI: XXV CICAT, 2016

Keywords: ethanol steam reforming; catalyst deactivation and regeneration; hydrogen production; nickel catalysts; cobalt catalysts; ceria.

Corresponding Author: Professor Vicente Cortés Corberán,

Corresponding Author's Institution: CSIC

First Author: Nicola Pinton

Order of Authors: Nicola Pinton; Mari Victoria Vidal; Arturo Martínez-Arias; Michela Signoretto; Vicente Cortés Corberán

Abstract: The catalytic behavior of nanostructured catalysts based on nickel, cobalt and cerium oxide in ethanol steam reforming (ESR) was studied to investigate the effect of the nature of the metal, their combination and the method of preparation. Mono- and bimetallic catalysts with equal metal content (M:Ce = 4:6, M = Ni, Co, or Ni/Co=1) were prepared by two methods, impregnation and coprecipitation within reverse microemulsions, characterized by SBET, XRD, TPO and HRTEM, and tested for ESR at 500°C. The nickel catalyst prepared from microemulsions exhibited the best performance in terms of catalytic activity (close to 100% conversion), stability and hydrogen yield. All the other catalysts deactivated at different paces due to formation of carbon deposits. The oxidative regeneration treatment of the deactivated catalysts recovered the initial activity of the impregnated catalysts but increased markedly those of catalysts from microemulsions. Thus, the catalytic behavior in ESR of the (Ni, Co)-Ce-O system depends on the preparation method, its composition and catalyst history.

Manuscript CATTOD-D-17-00073 Authors' replies to reviewers' comments:

Reviewer #1: In this work, authors tested the performance of nano-catalysts containing Ni, Co and Ce for ethanol steam reforming. This work is worthy of publication after revision as follows:

We thank the reviewer for his/her positive overall assessment

1) Please improve the usage of English.

Usage of English has been revised throughout

2) Introduction: Ethanol is a very good additive for liquid transportation fuel. Authors should explain the rationale for rather converting it to hydrogen.

The use of ethanol as fuel additive (in internal combustion engines) is out of the scope of this manuscript. Nevertheless we have included a sentence to address this matter in the introduction: Though it is a very good additive for liquid transportation fuel, the low energy efficiency of the internal combustion engines as compared to that fuel cells, makes preferable its transformation into hydrogen for its use in fuel cells.”

The authors' review of the literature is incomplete. Many useful reviews on ethanol steam reforming and past works on Ni and Co catalysts are missing!

Our cited ref. [3] includes and discusses most of the reviews on ethanol steam reforming prior to 2012 (Benito et al, 2005; Haryanto et al, 2005; Vaidya et al, 2006; Ni et al, 2007; Subramani and Song, 2007; Bshish et al. 2011; Bin et al, 2012) that were not mentioned separately to avoid duplication, and more recent reviews were referred to in the discussion (refs. [20] and [21]). Nevertheless, following reviewer's comment we have added four additional recent reviews (now [10,11,14,15]) and moved the previous citations of reviews [20] and [21] to the initial set of references (now [12, 13]) for the convenience of the readers.

Eqs. 3 to 13 are well documented in literature. Unless authors link their results to these, any repetition is superfluous.

We agree with the referee but they are used for discussing the catalytic performances and their evolution in Section 3. Nevertheless, we have re-written and simplified the whole paragraph in order to show the reaction network involved and the positive or deleterious effect of each reaction on hydrogen yield.

3) Section 2.4 is titled oxidation! No accuracy in measuring temperature and flow is stated. What was system pressure? Did authors check for error in measurements and consistency of results? Section 2.4 title has been corrected. Accuracy of temperature or flow measurements is guaranteed by the automatized equipment Microactivity Reference we used, which usage among catalytic laboratories is widespread, so we did not mention it. Nevertheless, following reviewer's

comments we have extended the description of the tests indicating accuracy, reaction pressure, error and consistency of measurements in the Experimental section

4) Fig. 3: Any comparison with past works on ESR for impregnated Ni and Co catalysts?

The catalytic performances of Ni and Co catalysts for ESR are extremely dependent on reaction conditions such as temperature, residence time, feed composition and ethanol-to-steam ratio; this implies that, for having a meaningful comparison with other catalysts, their corresponding catalytic tests should be conducted at practically equal reaction conditions. The dispersion of the tested reaction conditions reported in literature did not allow us making useful comparisons.

5) Section 3.3 should include a comparison with the results shown in section 3.2.

Such a comparison of the results of both sections constitutes the content of the discussion in Section 3.5.

6) Conclusions: Please highlight the best conditions for producing hydrogen.

As the objective of the work was comparison of catalytic performances we used a single set of fixed reaction conditions (feed composition, W/F, reaction temperature and pressure). So, we cannot make any conclusion on the best conditions for producing hydrogen, but only on which is the best performing catalyst among those we have investigated.

Reviewer #2: The manuscript "Ethanol steam reforming on nanostructured catalysts of Ni, Co and CeO<sub>2</sub>: influence of synthesis method on activity, deactivation and regenerability" was reviewed and some issues must be addressed before it is suitable for publication in the journal.

Authors described the behavior of Ni, Co and Ni-Co catalysts before and after the ethanol steam reforming, based on different methods of preparation. They also evaluated the catalysts regeneration process. Catalysts were characterized by SBET, XRD, TPO and HRTEM. Although the authors have a reaction dataset for a good discussion, there is not a good dataset of catalysts characterization before the reaction. Then, this is not possible to understand the behavior of the some catalysts, which compromise the quality of this work.

Certainly, the characterization of the fresh catalysts could be more substantiated. It is however our main aim to get general characteristics of the systems which we get from the results reported in Table 1 and figures 1 and 2, which allowed us to describe most relevant structural features of the as-prepared catalysts (crystalline phases, base metal atoms insertion in ceria network, textural properties). The exploration of other important properties like the analysis of the metal dispersion was discarded because of the nature of the systems which imposes important difficulties for such analysis (chemisorption procedures are not of help due to difficulties to discard adsorption from the support itself; direct analysis by techniques like TEM is not able to characterize dispersed metals due to the absence of contrast between components). It must be taken into account that our main aim is to study the differences between nickel and cobalt (and/or

bimetallic nickel-cobalt) in terms of their most relevant ESR catalytic properties and how different catalyst configurations (as attained by changing the preparation method) could affect to such properties. In any case, it can be noted we have extended the characterization of used systems by including new analysis by EDX in order to substantiate the discussion about activity/deactivation characteristics of the catalysts.

Abstract: authors said that the effect of the history of catalysts was observed, however it was not evaluated in the manuscript.

The content of the manuscript describes how the catalytic performance of each catalyst composition varies depending on the pretreatment, time on stream in ESR, reactivation treatment and again on time on stream of the regenerated sample, i.e., on the history of the sample, and discusses all those effects. That is what we meant in the abstract.

Is it possible to change the references 23 and 24 for indexed manuscripts?

We are sorry that the content of these references, corresponding to oral communications to a national congress, have not been yet published in indexed journal. Nevertheless, a new sentence describing the main features of their content has been inserted in the last paragraph of the introduction for convenience of the readers.

Selectivity is commented in the results, but the equation of selectivity was not presented.

We thank the reviewer to point out this. Equations of selectivity for carbon containing products and for hydrogen have been included in Experimental.

How many times were the experimental reactions repeated? Are the Results obtained with Ni-Co-CeO<sub>2</sub> (M) reproducible?

Catalytic tests were duplicated for all the impregnated catalysts, while those of catalysts prepared by microemulsion were repeated three times due to its unexpected behavior. Tests for each sample were reproducible within experimental error. A sentence stating this has been added to Experimental.

The effect of metal composition was not discussed.

We regret we may not understand this reviewer's comment as section 3.2 shows the effect of metal composition in impregnated catalysts and Section 3.3 the effect in impregnated catalysts, and the different effect of metal composition depending on the preparation method is discussed in Section 3.5.

The preparation of cerium oxide support by impregnation should be presented with more details. What were the quantities of compounds used ((NH<sub>4</sub>)<sub>2</sub>Ce(NO<sub>3</sub>)<sub>6</sub> · 6H<sub>2</sub>O) and urea) and what about solutions concentration? Was calcination of cerium under oxidant atmosphere? What was the heating rate?

This ceria support was prepared by the method described by Kundakovic and Flytzani-Stephanopoulos [J. Catal.179 (1998) 203-221], which reference has been now added for providing all the relevant details.

The procedure of reverse microemulsion needs to be better explained. Two solutions were prepared: the first with organic/cosurfactant/surfactant/aqueous; the second had organic/cosurfactant/surfactant/base. Is that correct? What was the quantity of each solution used?

The procedure is detailed in the cited reference [29]. Both microemulsions are of the same characteristics in terms of proportion of components. The only change is the components of the aqueous solution in each case: a solution of the metal precursor salts in the first one and a solution of the TMAH base in the second. This has been extended in the corresponding section of Experimental in order to clear this point.

Catalysts were not well characterized before the reaction. Then, it is not possible to understand what are the structural and morphological differences between the active phases of the catalysts. It would be important to understand the behavior of the catalysts during the reaction.

Certainly most relevant characterization of this type of systems is the one which is made under reaction conditions. Furthermore, characterization should point to analyze details taking place at the interfaces between active metallic forms of nickel or cobalt and the ceria support in each case, which is in any case a very complicated task. We appreciate the comment by the reviewer but however consider that getting such details falls somewhat out of the scope of present manuscript while work is in progress to cover this issue and as it will be considered for a future contribution.

The authors evaluated the catalysts after the reaction in relation to deactivation and regeneration. It were observed some interesting and unexpected results. For example, the unexpected effect of regeneration for Ni-Co-Ce (M) catalyst needs to be better studied and explained. What induced this behavior? Could it be the preparation method? If yes, it is necessary to be clarified.

Our results show clearly that this effect depends on the preparation method, which determines the dispersion of the active metal and its interaction with the support (see reply to next comment). Microemulsion coprecipitation can lead to a higher insertion of the active metals in the network of the ceria support, as shown by the absence of segregated Ni- or Co-containing phases in the bimetallic system prepared by microemulsion, which means that, at variance of NiCo-I, there is probably a random surface distribution of both metal atoms. Further than such insertion of the metals in the fluorite ceria lattice, product distribution over the fresh NiCo-M sample points to a majority of Co atoms on its surface in relative terms while over the regenerated sample, product distribution is more similar to that of Ni-M, which points out to a majority of Ni atoms on the surface. Our hypothesis is that the effect of reaction followed by oxidative regeneration importantly affects the evolution of the metals in this system while the

effect of a localized heating at the surface leads finally to Ni atoms “emerged” from the network, thus changing the catalytic behavior. Additional sentences have been added to Discussion to better describe our hypothesis in this sense.

What was the differences observed in the active phase obtained by the different preparation methods?

In principle, the active phase must be related in any case to the combination between metallic states of either nickel or cobalt and the underlying ceria support (more or less doped with nickel or cobalt heterocations), as also evidenced by XRD of the used samples. It is the physicochemical properties of such interfaces which must determine the ESR catalytic properties of the systems. The obtained results reveal in such sense that the generation of more intimate contacts between nickel and ceria in the system prepared by microemulsion can produce very active catalysts for the process. The presence of cobalt, further than showing some particular catalytic properties itself, generally affects such interaction in a detrimental way and the same apparently occurs when using impregnation as preparation method, most likely because of higher difficulties to establish most active interfacial configurations in such case.

Another question: it is important to observe that the hydrocarbons and alcohols steam reforming reactions occur on metallic catalysts and the active phase is the metal and not the metal oxide. Then, before the reactions, the catalysts are reduced to metallic phase, normally using hydrogen as reduction agent. In this work, the authors did not use this procedure and the catalysts were activated over an oxidant atmosphere. However, it is possible to the metal reduction to occur during the reaction, but it is important that the authors explain it clearly. Why did they decide to do it this way?

The pretreatment in pure hydrogen at high relatively high temperature may cause metal sintering, reducing metal dispersion. However a reduction by a softer reductant (as ethanol, for example, or, in fact the ESR reactant mixture) may allow keeping the initial cation dispersion in the oxidic precursor. As the activity of catalysts containing ceria is strongly dependent on the number of vacancies in its network, which in turn are dependent not only on the preparation method but also on its contact with environment and its storage. For these reasons we used oxidative activation to homogenize the initial oxidation state of ceria in the catalysts, and the reduction of the active metal component takes place by its interaction with the reaction medium. This has been observed in other metallic systems: Zeolite-supported nanosilver catalysts used for CO oxidation at low temperatures show much higher activity if they are pretreated consecutively first with oxygen and then with reduced with hydrogen than if they are just reduced in hydrogen [E. Kolobova et al., Fuel 188 (2017) 121-131]. A new paragraph and this reference has been added in Section 3.5.

It is weird that in the first few minutes of reaction the conversion has been 100% or near 100%. If this occurs, the activation of catalysts with hydrogen is unnecessary, and this is an important result.

Regardless of the catalyst activation procedure, total conversion could result from a variety of reaction conditions such as an excess of residence time for the reaction temperature used or a temperature too high for a given residence time. So, this result “per se” does not mean that activation with hydrogen is unnecessary.

Let us point out that our test conditions were selected to obtain an initial conversion as high as possible, but without reaching full conversion, in order to be able to observe big variations if they would occur.

Then, what is the active phase in the first minutes of reaction?  $\text{Ni}^{2+}$ ,  $\text{Ni}^0$ ,  $\text{Co}^{2+}$ ,  $\text{Co}^0$  ? and what is the mechanism of reaction?

Prior to reaction Ni and Co are in the  $2+$  state as shown by the fresh catalysts characterization, and the oxidation pretreatment excludes their reduction before contacting the reaction medium. As the active centers must basically correspond to the metallic state (as confirmed by used catalysts characterization), one may infer that both cations are reduced by the ethanol in the reactant mixture during the initial moments of their contact.

As our first product analysis is made after at least 15-30 minutes of the initial contact, the product distribution corresponds to catalytic ESR. This reasoning has been incorporated to discussion in Section 3.5.

Lines 207-211: This text is confusing, because when the catalyst contains only Ni or Co, the lattice parameter  $a$  of ceria increased, and it was due to reduced state of cerium in network. But, when the catalyst contains Ni and Co the lattice parameter  $a$  decreased and it was attributed to cerium oxidation.

The insertion of divalent cations in the network of ceria is typically proposed to occur through substitutional exchange with cerium cations. Such exchange requires the formation of oxygen vacancies for keeping charge neutrality in the lattice. On the whole, and despite the fact that oxygen vacancy formation can lead to a certain expansion of the lattice as a consequence of increased repulsion between cations, the lower ionic radius of the divalent (or trivalent) nickel or cobalt cations with respect to  $\text{Ce}^{4+}$  produces a lattice contraction upon mentioned substitutional incorporation. On the other hand, the reduction of  $\text{Ce}^{4+}$  to  $\text{Ce}^{3+}$  also has to be accompanied by oxygen vacancy formation while the ionic radius becomes increased and both effects lead to lattice expansion. Interpretation of the evolution of lattice parameters is made on these bases.

This broader description has been added to the corresponding paragraph in the text body

When the catalysts-I were regenerated, they showed a different trend in contrast with the fresh ones. This result needs to be more explored. What is happening?

The overall trend of deactivation for each sample was similar for the fresh and the regenerated state of each catalyst. Nevertheless, as mentioned above, we believe that main catalytic difference as a function of the preparation method is related to the fact that the microemulsion method may give rise to more intimate contact between nickel and the support. In addition to achieving most likely lower degree of metal dispersion through impregnation, the interfacial structure could also be different in each case. On the whole, all these aspects are believed to affect the differences observed

The catalyst Ni-Ce (M) was better than the other catalysts. Why did it happen? What was responsible for this behavior? Which was the difference observed in the active phase of this catalyst when compared with the others?

We believe that the interaction of components nickel and ceria becomes maximized in such case. First, the microemulsion preparation allows a more intimate contact between components. Second, the absence of cobalt allows maximizing mentioned interactions.

Acetaldehyde was not observed in the reaction with Ni-Ce (M) catalyst?

Formation of acetaldehyde was observed on each catalyst, but its yield on Ni-Ce (M) catalyst was so small it can be considered negligible. This implies that reforming of acetaldehyde on its catalysts is faster than its formation from ethanol.

Ni-Ce (M) catalyst not showed formation of acetone and ethylene.

Co-Ce (M) catalyst was the responsible by the formation of acetone and ethylene.

And, Ni-Co-Ce (M) showed higher formation of them.

Why? What is the explanation?

Nickel is much more active than cobalt to activate ethanol, which is the first step in the overall process. Thus, the higher formation of acetone and ethylene on the fresh NiCo-M catalysts compared to that of fresh Co-M could be due to the easier activation of ethanol on nickel while the product distribution is controlled by cobalt.

"Emergence" of the active metal atoms can be evaluated within situ techniques, as XAS, XPD, and it must be done before publishing this manuscript.

We appreciate the reviewer's suggestion but, as mentioned above, completing the work in the mentioned sense falls somewhat out of the scope of the present work and will in any case be object of another paper under preparation. Nevertheless, we have added EDX analysis of the regenerated NiCo-M sample after use in ESR that shows a surface enrichment in Ni, which is coherent with our hypothesis.



The explanation presented in lines 332-336 is only speculative.

We agree we do not have sufficient evidences for mentioned proposal but we are just posing such explanation as a possible hypothesis. The whole paragraph of explanation has been re-phrased to underline the hypothetical nature of our interpretation.

## LIST OF THE MODIFICATIONS MADE

(all these changes are highlighted in red in the revised manuscript)

Usage of English has been revised throughout

### Introduction:

New sentences considering the use of ethanol as fuel additive are included (1.54-56)

Paragraphs concerning the reaction network have been simplified, re-ordered and re-written (1.62-83)

Four new references to ESR reviews have been added.

Description of preliminary results has been expanded (1.113-115)

### Experimental:

A new reference and more details are included in catalyst preparation, and EDX details have been added.

Details of temperature and flow precision, reproducibility of results, carbon balance, and the formulae for selectivity of products have been added

### Section 3.1

Discussion on interpretation of cell parameter changes has been expanded (1.218-224)

### Section 3.4

Discussion of XRD results have been partially re-phrased to give additional details (1.268-278)

New data from EDX have been added in New Table 2, and a paragraph discussing them has been added (1.309-317)

### Section 3.5

New paragraphs describing the choice of activation treatment (1.319-338) and on the effect of preparation method and metal composition (1.339-348) have been added.

Discussion on the effect of the reaction –regeneration cycle on NiCo-M catalyst have been re-written (1.377-391)

### Conclusions

A new paragraph has been added (1.425-428)

### Acknowledgement

A new line has been added

### References

7 new references have been added and the numbering corrected accordingly.

Table 2 has been added



## HIGHLIGHTS

Synthesis by reverse microemulsions makes more efficient catalysts than impregnation

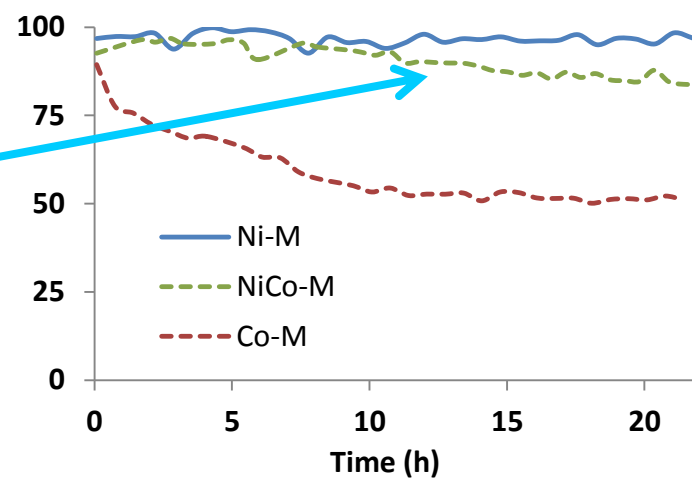
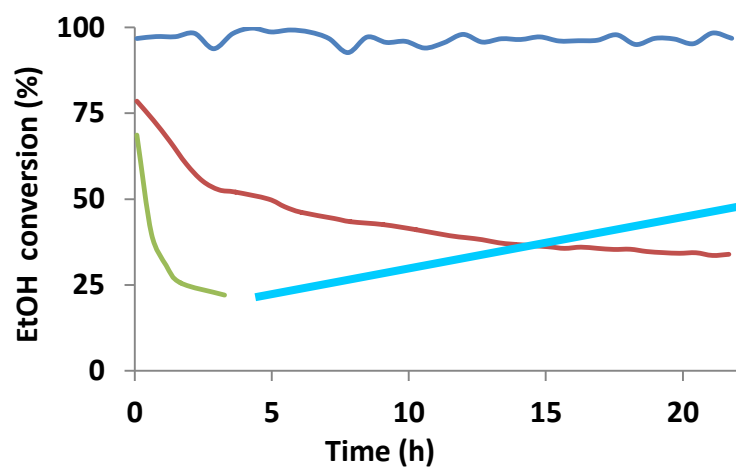
Catalytic activity and stability depend on the metal and the synthesis method

Deactivated catalysts activity can be regenerated by oxidative treatment

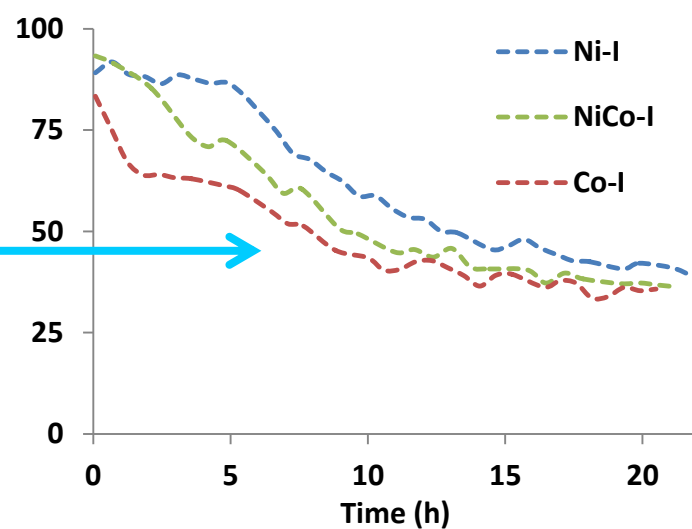
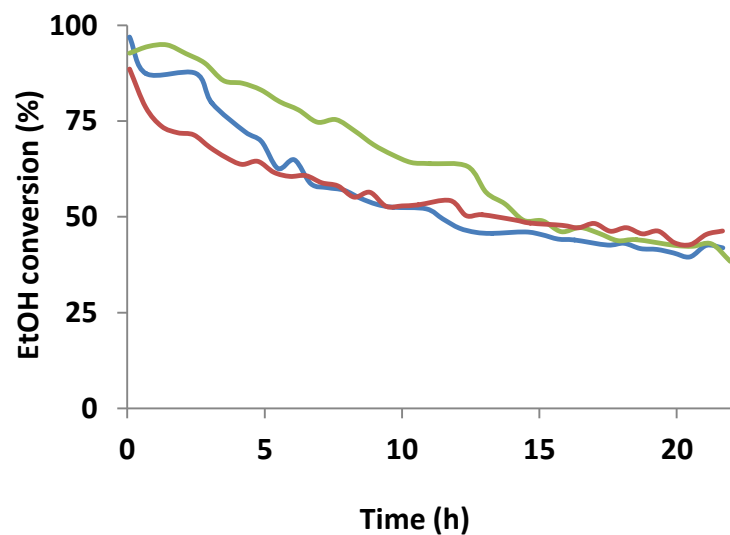
Synthesis method influences nature of deposited carbon and catalyst regenerability

Unexpected effect of regeneration found for bimetallic NiCo-CeO<sub>2</sub> catalyst

## Catalysts from microemulsions ( *M* )



**REGENERATION**



## Impregnated catalysts ( *I* )

1 Ethanol steam reforming on nanostructured catalysts of Ni, Co and CeO<sub>2</sub>:  
2 Influence of synthesis method on activity, deactivation and regenerability

3  
4 N. Pinton<sup>a,b</sup>, M.V. Vidal<sup>b,c</sup>, M. Signoretto<sup>a</sup>, A. Martínez-Arias<sup>b</sup>, V. Cortés Corberán<sup>b,\*</sup>

5 <sup>a</sup> Department of Molecular Sciences and Nanosystems, Università Ca' Foscari, Venezia, Italia

6 <sup>b</sup> Institute of Catalysis and Petroleumchemistry (ICP), Spanish Council for Scientific Research  
7 (CSIC), 28049 Madrid, Spain.

8 <sup>c</sup> LICATUC, Universidad de Cartagena, Cartagena de Indias, Colombia

9 \*e-mail: [vcortes@icp.csic.es](mailto:vcortes@icp.csic.es)

10

11 **Abstracts**

12 The catalytic behavior of nanostructured catalysts based on nickel, cobalt and cerium oxide in  
13 ethanol steam reforming (ESR) was studied to investigate the effect of the nature of the metal, their  
14 combination and the method of preparation. Mono- and bimetallic catalysts with equal metal content  
15 (M:Ce = 4:6, M = Ni, Co, or Ni/Co=1) were prepared by two methods, impregnation and  
16 coprecipitation within reverse microemulsions, characterized by S<sub>BET</sub>, XRD, TPO and HRTEM,  
17 and tested for ESR at 500°C. The nickel catalyst prepared from microemulsions exhibited the best  
18 performance in terms of catalytic activity (close to 100% conversion), stability and hydrogen yield.  
19 All the other catalysts deactivated at different paces due to formation of carbon deposits. The  
20 oxidative regeneration treatment of the deactivated catalysts recovered the initial activity of the  
21 impregnated catalysts but increased markedly those of catalysts from microemulsions. Thus, the  
22 catalytic behavior in ESR of the (Ni, Co)-Ce-O system depends on the preparation method, its  
23 composition and the catalyst history.

24

25 **Keywords:** Ethanol steam reforming, hydrogen production, nickel, cobalt, bimetallic catalysts,  
26 reverse microemulsions, catalyst deactivation, catalyst regeneration

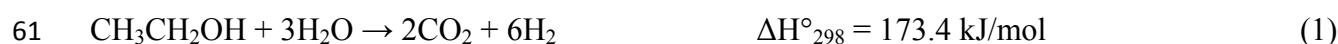
27

28 **1. Introduction**

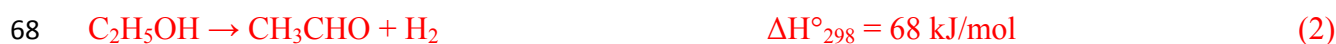
29 The environmental impact of the massive use of fossil fuels on the emission of greenhouse gases  
30 requires the restructuring of existing energy systems, a major technological development of new  
31 alternatives and the use of new, cleaner energy carriers. In this framework, hydrogen can play a  
32 crucial role as a clean fuel (in combustion engines and fuel cells) in addition to its use as raw  
33 material in the Chemical Industry [1]. Hydrogen is mainly consumed in oil refining processes,

34 ammonia and methanol synthesis and employed as fuel only in spaceships and in some vehicle  
35 prototypes. Promising technologies like fuel cells allow converting the chemical energy contained in  
36 the H-H bond in electric energy through the clean combustion of H<sub>2</sub> in presence of an oxidant.  
37 However, to extend these promising and clean technologies to a large scale, some issues linked with  
38 hydrogen physical and chemical properties must be considered. Hydrogen is a very light gas, non  
39 toxic, colourless, but easily flammable in air in the range of concentrations 4-75% by volume. It has  
40 a low energy density on a volume basis (gasoline density is 0.7 kg/L whilst H<sub>2</sub> density is 0.03, 0.06  
41 and 0.07 kg/L at 350 atm, 700 atm and liquefied (20 K), respectively). So, it is clear that hydrogen  
42 economy needs safe and cheap storage systems or, alternatively, technologies to produce it *in situ* (or  
43 on board for mobile uses) from easily transportable liquids. On the other hand, currently hydrogen is  
44 mostly produced from fossil fuels in processes like methane steam reforming or coal gasification;  
45 this means that, though hydrogen combustion is clean, the overall cycle (hydrogen production -  
46 hydrogen combustion) involves no reduction of CO<sub>2</sub> emissions. Thus, the reduction of the  
47 environmental impact thanks to its use as energy vector requires hydrogen to be produced from  
48 renewable resources. This makes biomass a promising resource for generating hydrogen through an  
49 easily scalable production process, because it is renewable and continuously available [2]. In this  
50 frame, ethanol can play an important role [3]. Ethanol, when obtained by biomass fermentation, is a  
51 renewable resource and about 95% of ethanol produced in the world comes from agricultural  
52 products, mainly from edible plants like sugarcane, sugar beet and corn [4, 5]. It has a high  
53 hydrogen-to-carbon ratio (H/C = 3) and high hydrogen content per unit of volume in the liquid state.  
54 Ethanol is a very good additive for liquid transportation fuel, the lower energy efficiency of the  
55 internal combustion engines as compared to that of fuel cells, makes preferable its transformation  
56 into hydrogen for its use in fuel cells.

57 Among the various catalytic pathways that can be used to produce hydrogen from ethanol, ethanol  
58 steam reforming (ESR) is an efficient and cost-effective technology [6] that gives the highest  
59 hydrogen production per ethanol molecule, as it extracts hydrogen not only from ethanol but also  
60 from water:



62 However, in spite of the apparent simplicity of its stoichiometry, ethanol reforming follows a  
63 complex reactive scheme which, in addition to H<sub>2</sub> and CO<sub>2</sub>, can give rise to a large number of by-  
64 products such as CO, ethylene, acetaldehyde and CH<sub>4</sub> among others, due to other simultaneous  
65 reactions which negatively affect the selectivity to hydrogen [3, 7]. Thus, ethanol, as an alcohol, can  
66 go through the dehydrogenation to acetaldehyde (2) and dehydration to ethylene (3) even at low  
67 temperatures:



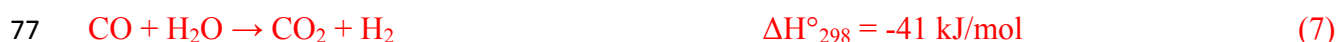
70 While ethylene represents the main precursor of coke, acetaldehyde plays an important role in the  
71 pathways leading to hydrogen formation through reforming:



74 CO formation by this latter reaction leads to lower hydrogen production from ethanol:



76 though additional hydrogen can be recovered via water gas shift (WGS):



78 In addition, acetaldehyde decomposition to methane (7) or condensation to acetone (8), and  
79 methanation (9):



83 decrease the hydrogen yield, what must be avoided by the catalysts. Furthermore, polymerization of  
84 ethylene and polycondensation of acetone can lead to coke formation, causing catalyst deactivation.  
85 This complexity requires the catalysts to be polyfunctional to direct the process to a maximum  
86 hydrogen yield and selectivity, as they have to break the C-C bond at relatively low temperatures, to  
87 keep low the production of CO, to resist the deactivation caused by coke deposition, to be stable in  
88 operative conditions and to limit the hydrogenation of the products. In addition, their practical  
89 application requires that catalysts may be regenerated after the almost unavoidable catalyst  
90 deactivation.

91 Many catalytic systems are active for ESR [3, 8-15], based on both noble metals (Rh, Pt and Pd) [8,  
92 9] and on transition metals (Ni, Co, Cu-Ni) [14,15]. The lower cost of the latter makes them an  
93 attractive alternative as Ni and Co show catalytic performance and stability comparable with those of  
94 the best noble metal systems. [16]. Bimetallic catalysts have the main goal to create a synergy of  
95 positive effects of two non-noble metals. Many combinations can be found in literature, like Fe-Co  
96 [17], Co-Cu [18] or Ni-Cu [19], supported on a variety of supports.

97 The role of the support is fundamental. Acid solids like  $Al_2O_3$  promote the dehydration of ethanol to  
98 ethylene, the most common coke precursor [20, 21], while basic supports like MgO are way more  
99 resistant to coke deposition, but generate more oxygenate products [22]. Redox supports like  $ZrO_2$   
100 and  $CeO_2$  have a high oxygen storage capability, high oxygen mobility and are active in the WGS  
101 reaction [23-25]. On the other hand, sintering of metal nanoparticles also causes irreversible catalyst



102 deactivation. This phenomenon is due mainly to a local and rapid temperature increase and in this  
103 process the role of the support is also significant. Acid supports have been reported to promote in  
104 particular Ni sintering, while redox supports, and in particular CeO<sub>2</sub>, give an increased thermal  
105 stability to the metallic phase [12].

106 The preparation method influences the textural properties, such as specific area, structural features  
107 like crystalline phases, and also activity, stability and life of the catalysts. Previous studies of copper-  
108 ceria catalysts for preferential CO oxidation (PROX) have found that support surfaces with different  
109 nature and interaction with the active phase can be produced by impregnation of ceria and by  
110 coprecipitation of the two components within reverse microemulsions, method that allows obtaining  
111 nanostructured systems with high structural, morphological and chemical homogeneity [26].

112 The preliminary results obtained for ESR with Ni-Ce-O and Co-Ce-O catalysts prepared in reverse  
113 microemulsions were promising [27, 28], showing that both systems were active with maximum  
114 activity for atomic ratio Ce/M = 6/4 for both systems (M = Ni, Co), and while Ni-Ce-O catalysts  
115 were more active, Co-Ce-O catalysts showed a very low formation of CO. This motivated the present  
116 study on the combination of both active metals (Ni and Co) with cerium oxide, as bimetallic Ni-Co  
117 may combine the ability of nickel to break C-C bond with the cobalt resistance to coke deposits [17-  
118 19]. We have investigated the influence of the preparation method on the activity, hydrogen yield,  
119 catalyst deactivation and regeneration of the bimetallic catalysts Ni-Co on ceria and compared them  
120 with their monometallic counterparts, and with their homologues prepared by wet impregnation. It  
121 has been found that the effect of both metals is not additive, and that the catalytic behavior strongly  
122 depends on the metal composition, the method of preparation and the history of the catalyst.

123

## 124 **2. Experimental**

### 125 2.1 Catalysts preparation

126 Two series of catalysts with equal chemical compositions (atomic ratio Ce/M = 6/4; M = Ni, Co or  
127 Ni-Co in a ratio Ni/Co = 1) were prepared using two different methods: wet impregnation (*I*) and  
128 coprecipitation in reverse microemulsions (*M*) [29]. In the first case, cerium oxide was chosen as a  
129 support for the active phase of nickel oxide and cobalt oxide. In the second, cerium is present in the  
130 structure of the mixed oxide system with the two non-noble metals.

#### 131 *A) Impregnation (I)*

132 Ni(NO<sub>3</sub>)<sub>2</sub>·6H<sub>2</sub>O 99% and Co(NO<sub>3</sub>)<sub>2</sub>·6 H<sub>2</sub>O 99% (Sigma-Aldrich) were used as metal precursors.

133 Cerium oxide support was prepared mixing aqueous solutions of (NH<sub>4</sub>)<sub>2</sub>Ce(NO<sub>3</sub>)<sub>6</sub>·6H<sub>2</sub>O and urea at  
134 100°C following the method described by Kundakovic and M. Flytzani-Stephanopoulos [30]. The  
135 precipitate was then filtered, washed with deionized water and dried overnight at 110 °C. The solid

136 was then ground and calcined in a tubular oven at 500 °C. Metals were incorporated by wet  
137 impregnation of calcined CeO<sub>2</sub> with an aqueous solution of the metallic precursor in the proper  
138 concentration in order to obtain the desired loading in a flask under inert atmosphere of nitrogen, to  
139 avoid CeO<sub>2</sub> carbonation. The suspension was kept gently stirring overnight. The exceeding water  
140 was removed and ultimately the samples were calcined at 500 °C for 4 h.

#### 141 B) Reverse microemulsion (M)

142 The reverse microemulsion was prepared with n-heptane 99% as the organic phase, 1-hexanol 98%  
143 as cosurfactant, and Triton X-100 Sigma Pro as non-ionic surface surfactant (all from Sigma-  
144 Aldrich). Ce(NO<sub>3</sub>)<sub>3</sub>·6H<sub>2</sub>O 99% (Aldrich Chemistry), Ni(NO<sub>3</sub>)<sub>2</sub>·6H<sub>2</sub>O 99% (Sigma Aldrich) and  
145 Co(NO<sub>3</sub>)<sub>2</sub>·6 H<sub>2</sub>O 99% (Assay) were used as metal precursors and (CH<sub>3</sub>)<sub>4</sub>N(OH) (TMAH) 25% w/w  
146 (Alfa Aesar) as base. The volume ratio organic/cosurfactant/surfactant/aqueous was 66/14/13/7 in all  
147 the preparations.

148 Organic phase, cosurfactant and surfactant were mixed with the aqueous solutions of the metals salts  
149 to produce the saline microemulsion. Similarly, basic microemulsion with the same proportion of  
150 components was prepared by replacing the aqueous solution of the metal salts with the TMAH one.  
151 Both microemulsions were stirred at 100 rpm for 1 h. Then, basic microemulsion was added slowly  
152 to the saline microemulsion to avoid abrupt changes in the pH. The resulting mixture was stirred at  
153 100 rpm for 24 h (oxides precipitation occurred in this time). After centrifugation and washing with  
154 methanol, the precipitate was dried overnight at 120°C and calcined in air at 500°C for 2 h.

155 Hereinafter catalysts are denoted with the component metal elements, followed by an “I” (if they  
156 were prepared by impregnation) or an “M” (if prepared by microemulsion).

#### 157 2.3 Catalyst characterization

158 The specific surface area ( $S_{\text{BET}}$ ) and pore volume were measured by the analysis of N<sub>2</sub> adsorption  
159 isotherms at -196 °C by a Micromeritics ASAP 2010 equipment. X-ray diffractograms were  
160 obtained on a Seifert XRD 3000P diffractometer using nickel-filtered Cu K $\alpha$  radiation operating at  
161 40 kV and 40 mA, using a 0.02° step size and 2 s counting time per point. Analysis of the diffraction  
162 peaks was done with the software ANALYZE Rayflex Version 2.293. Temperature programmed  
163 oxidation (TPO) experiments were conducted in a quartz reactor, using a flow of 5% O<sub>2</sub> in He and a  
164 heating rate of 10 °C/min, and analyzing the effluent gases by means of a quadrupole mass  
165 spectrometer Pfeiffer Vacuum OmniStar™. High resolution transmission electron microscopy  
166 (HRTEM) tests were made at a TEM/STEM instrument JEOL 2100F operating at 200 kV with a  
167 Field Emission Gun (point resolution: 0.19 nm), which has an attached energy-dispersive X-ray

168 spectroscopy (EDX) detector INCA x-sight (Oxford Instruments) for semiquantitative chemical  
169 analysis.

## 170 2.4 Catalytic tests

171 Catalysts were tested for ESR at 500 °C and near atmospheric pressure, with a feed of molar  
172 composition water:ethanol:He = 18.4:3.1:78.5 and W/F = 0.12 g<sub>cat</sub>.h/mol ethanol, in a stainless steel,  
173 fixed bed tubular reactor placed in an equipment Microactivity Reference model MAXXXM3 (PID  
174 Eng & Tech) which allows controlling the reaction temperature within ± 1°C thanks to a coaxial  
175 thermocouple placed in the center of the catalytic bed. Reactants flows were controlled by mass flow  
176 controller with a precision of ± 1% of full scale. Prior to the reaction, fresh (unused) catalyst samples  
177 were activated under flow of 10% O<sub>2</sub> diluted in He, at 650 °C for 1 h. Catalytic stability tests were  
178 conducted at 500°C for 22 hours. After the first run, if the catalyst suffered a deactivation, it was  
179 cooled down and flushed under inert flow, and then reactivated using the same procedure of the  
180 initial activation, i.e., heating up to 650 °C at 10 °C/min and keeping this temperature for 1 h, under a  
181 flow of 10% O<sub>2</sub> in He. Then, after cooling down to 500 °C in inert flow, a second run was conducted  
182 with the regenerated samples under the same conditions of the first run. Catalytic tests were  
183 duplicated for all the impregnated catalysts, while those of catalysts prepared by microemulsion  
184 samples were repeated three times due to its unexpected behavior. Tests for each sample were  
185 reproducible within experimental error. Carbon balance in the reported data were within 100 ± 5%  
186 Reactants and products were analyzed on line by GC on a Varian Star 3400 CX instrument equipped  
187 with two columns, one filled with molecular sieve (for H<sub>2</sub>, CO and CH<sub>4</sub>) and other with Porapak Q  
188 (for the rest of compounds), and a thermal conductivity detector.

189 Yield (Y<sub>i</sub>) and selectivity (S<sub>i</sub>) of carbon-containing products and ethanol conversion (X<sub>EtOH</sub>) were  
190 calculated on a C atom basis and expressed as mol%:

$$191 \quad Y_i = \frac{f_i \cdot nC_i}{2f_{\text{EtOH in}}} \cdot 100 \quad X_{\text{EtOH}} = \sum Y_i \quad S_i = Y_i / X_{\text{EtOH}}$$

192 where  $nC_i$  is the number of C atoms contained in the product  $i$  and  $f_i$  is its molar flow (mol/h).

193 According to the stoichiometry of the reforming reaction (1), the maximum possible yield of  
194 hydrogen is 6 mol H<sub>2</sub>/mol ethanol; therefore hydrogen yield (Y<sub>H<sub>2</sub></sub>) and selectivity (S<sub>H<sub>2</sub></sub>) were  
195 calculated (in mol%) as:

$$196 \quad Y_{\text{H}_2} = \frac{f_{\text{H}_2 \text{ out}}}{6 \cdot f_{\text{EtOH in}}} \cdot 100 \quad S_{\text{H}_2} = \frac{f_{\text{H}_2 \text{ out}}}{6 \cdot (f_{\text{EtOH in}} - f_{\text{EtOH out}})} \cdot 100$$

197

## 198 **3. Results and discussion**

### 199 3.1 Catalyst characterization

200 Table 1 summarizes the results of  $S_{\text{BET}}$  and average pore diameter. All catalysts could be classified as  
201 mesoporous materials, as they all show a type IV isotherm with H2 hysteresis (not shown), but  
202 impregnated catalysts (I) presented a multimodal pore size distribution in contrast with the unimodal  
203 distribution of the (M) samples **from microemulsions**.

204 X-ray diffraction patterns of all fresh samples (Fig 1 y 2) showed the characteristic reflections of the  
205 fluorite-like cubic phase of  $\text{CeO}_2$ , with similar intensity and width within each series. Table 1 also  
206 shows the lattice constant and size of the crystals calculated from the analysis of the most intense  
207 diffraction, **corresponding to** the (111) plane of this  $\text{CeO}_2$  cubic phase. The patterns of the  
208 impregnated catalysts (Fig. 1) show sharper and more intense peaks, meaning that the particles of the  
209 support are bigger and more crystalline, while the preparation via microemulsions leads to more  
210 amorphous materials (Fig. 2); nevertheless, within each series there were no meaningful differences  
211 in crystal sizes. The diffractograms of monometallic catalysts Ni-I and Co-I evidenced also the  
212 presence of the cubic phases  $\text{NiO}$  and  $\text{Co}_3\text{O}_4$ , respectively, while bimetallic NiCo-I contained  
213  $\text{NiCo}_2\text{O}_4$  and  $\text{NiO}$  phases. Ceria crystalline particles **were** smaller and less crystalline in the (M)  
214 samples but the phase composition of the homologous catalysts was similar in both series, excepting  
215 sample NiCo-M which pattern did not present any diffraction lines that could be assigned to nickel or  
216 cobalt containing compounds. The lattice parameter  $a$  of ceria increased in all the monometallic  
217 catalysts in relation to that of the pure ceria phase (0.541 nm), which suggests that cerium is in a  
218 partially reduced state in the network: **the reduction of  $\text{Ce}^{4+}$  to  $\text{Ce}^{3+}$  leads to lattice expansion because**  
219 **of the increase in the ionic radius as well as the fact that it has to be accompanied by oxygen vacancy**  
220 **formation**. Catalysts NiCo-M and NiCo-I showed slightly lower lattice parameter values, probably  
221 due to the **insertion of** heterocations, either of Ni or Co, into the ceria network probably **through**  
222 **substitutional exchange with cerium cations; the lower ionic radius of the divalent (or trivalent)**  
223 **nickel or cobalt cations with respect to  $\text{Ce}^{4+}$  produces a lattice contraction that may compensate the**  
224 **network expansion expected upon associated formation of oxygen vacancies**.

### 225 3.2. Catalytic performance of impregnated catalysts

226 Preliminary tests, conducted in the range 400-650 °C, showed **all catalysts deactivated but each one**  
227 **with a different pace**. Thus, we selected the temperature of 500 °C to study and compare the catalytic  
228 performance and stability in isothermal experiments for 22 h. Under the tested conditions, reaction in  
229 the absence of catalysts reached an ethanol conversion  $< 6\%$  with  $Y_{\text{H}_2} < 1\%$ .

230 Figure 3 shows the effect of run time on ethanol conversion and hydrogen yield of ESR on the  
231 impregnated catalysts (I). The three showed a high initial activity (near total conversion) but suffered  
232 a gradual deactivation for the first 15 hours, and later the values of conversion remained similar for

233 the three catalysts (45-50%) and deactivation was slower. Evolution of the hydrogen yield was  
234 parallel to that of conversion (fig. 3), indicating that deactivation was not affecting the hydrogen  
235 selectivity (around 60%). The bimetallic NiCo-I was the most active, selective and stable catalyst,  
236 with 95% ethanol conversion and  $Y_{H_2} = 59\%$  after 1.5 h, and keeping values above 63% conversion  
237 and 37% hydrogen yield for about 12 h.

238 TPO tests of the used samples (Section 3.4) evidenced the presence of carbon deposits on them. As  
239 this coke deposition was considered the most probable cause of the activity loss, to regenerate their  
240 catalytic activity, the used samples were submitted to oxidative reactivation in order to clean the  
241 surface by burning the deposited carbon that covered pores and active phases. After this treatment,  
242 initial conversion values were similar to those of the fresh samples, but the reactivated samples  
243 showed a different order of activity than the fresh ones (Fig. 4): the Ni-I was the most active,  
244 selective and stable, keeping the order along the run time: Ni-I > NiCo-I > Co-I. Anyway, reactivated  
245 samples also suffered deactivation and the overall deactivation trend shown was parallel to that of  
246 their fresh samples, so further characterizations were conducted on these used catalysts.

### 247 3.3. Catalytic performance of catalysts from microemulsions

248 Coprecipitated catalysts prepared via microemulsions displayed a quite different behavior and  
249 evolution under the same operative conditions (Fig. 5). Ni-M was the most active and stable catalyst,  
250 as it kept conversion above 95% and near constant hydrogen yield around 57% (equivalent to 3.4  
251 mol H<sub>2</sub>/mol ethanol) during the 22 h of our test. Fresh Co-M showed a lower initial conversion, and  
252 deactivated following the same evolution than its impregnated equivalent Co-I, but with lower  
253 performance: some 15-20 percentage points of conversion less at equal run times. After regeneration  
254 treatment, the reactivated Co-M sample showed similar initial activity than the fresh one, but it  
255 became more stable, losing only 10% of its activity (vs. a 40% loss for the fresh sample) after 7 h  
256 and remaining practically stable thereafter.

257 The catalytic behaviour of NiCo-M was unique: the fresh sample showed the lowest initial activity  
258 and quickly deactivated in 3 hours. This lowest initial activity could be related to a limited  
259 accessibility to Ni and/or Co atoms, as XRD showed this was the only catalyst for which no  
260 segregated oxide phases of Ni or Co were detected (Fig. 2) while showing the lowest lattice  
261 parameter in its ceria fluorite phase (Table 1). But, surprisingly, after the reactivation treatment it  
262 became almost as active as the most active one, Ni-M, as its ethanol conversion was very high, above  
263 85%, and remained stable for 22 hours. Hydrogen yields trends were parallel to that of the ethanol  
264 conversion: reactivated NiCo-M and Ni-M were also the most selective catalysts with  $Y_{H_2} > 56\%$  for

265 22 h of reaction (Fig. 5). These results point to a restructuring of its surface and/or active centers  
266 caused by the regeneration process.

#### 267 3.4. Characterization of the used catalysts

268 XRD patterns of all the used catalysts, independently from the preparation method, presented  
269 reflections attributable to carbon species, probably with a graphite-like structure (Fig. 6). In all cases,  
270 after the activation and use in the ESR test the crystal particle size of the CeO<sub>2</sub> phase increased and  
271 the oxidic phases of the active metals were reduced to the respective zero state metals. In the  
272 impregnated bimetallic sample NiCo-I only the diffraction lines of Ni<sup>0</sup> can be identified, while no  
273 evidence of crystalline cobalt can be found. Used Ni-M sample was fully active after 22 hours, when  
274 the test was stopped; so, considering its XRD pattern, it can be concluded that Ni<sup>0</sup> particles may be  
275 the real active phase, responsible of the catalytic performance of this catalyst. It can be reasonable to  
276 think that the nickel reduction occurred at the beginning of the ESR test and may be caused by the  
277 reduction of the precursor oxide with ethanol in the reactant mixture while the presence of hydrogen  
278 produced by ESR can also help to maintain the reduced state of nickel.

279 The evolution of CO<sub>2</sub> during the TPO (5% O<sub>2</sub>/He) of the used catalyst samples was monitored, and  
280 the resulting CO<sub>2</sub> profiles evidenced different types of carbonaceous species with different thermal  
281 stabilities (Fig. 7). Both Co-containing impregnated catalysts profiles show a very broad and intense  
282 peak in the range 525-700 °C, with maxima at 625 and 700 °C for NiCo-I, along with minor peak at  
283 lower temperature (500 °C), while the Ni-I profile showed only the broad peak at 700 °C. This peak,  
284 present in the three profiles, indicates that the same type of carbonaceous compounds, with relatively  
285 strong thermal stability, was deposited on the surface of the samples during ESR. For NiCo-I the  
286 predominant contribution is the peak at 620 °C, probably corresponding to polymeric non-structured  
287 coke species, with a weaker interaction with the catalytic surface. The minor peaks around 500 °C  
288 can correspond to the decomposition of carbonates stabilized during ESR reaction.

289 TPO profiles of the used catalysts from microemulsion are quite different and show basically two  
290 peaks at 550°C and 630°C. The first peak is predominant, so this corresponds to the main  
291 carbonaceous compounds formed on the catalysts during the reforming reactions, which could  
292 correspond to carbon filaments, as confirmed by further TEM analysis. Figure 8; **Error! No se  
293 encuentra el origen de la referencia.** shows two TEM images obtained for the used Ni-I sample.  
294 The nickel particles can be discriminated due to their stronger contrast. The light grey structures have  
295 been attributed to the carbonaceous species. A large presence of amorphous carbon can be identified  
296 along with a small portion of carbon nanotubes. The TPO peak at higher temperatures, corresponding  
297 to the type of carbon deposit with the strongest interaction with the catalyst, may be attributed to this

298 amorphous polymeric carbon compound that seems to block the metal particles, limiting the access  
299 to the active sites with a consequent loss of activity. Another relevant contribution to the catalyst  
300 deactivation can be assigned to the sintering of nickel particles which appear bigger in the used  
301 sample than in the fresh one.

302 On the contrary, in the used Ni-M catalyst prepared from microemulsions the nickel particles  
303 remained well dispersed and with an average dimension of 10 nm (Fig. 9). These morphological  
304 properties may be linked to the high stability, activity and selectivity of these samples in the reaction  
305 as it must be remembered that Ni-M did not experience any deactivation after 22 hours. This sample  
306 exhibits a lower amount of carbon which appears mainly as nanotube structures along with a small  
307 amount of amorphous coke. However, these carbonaceous deposits did not affect the catalytic  
308 performance of this sample probably because carbon nanotubes do not block the access to the active  
309 phase as non-structured coke do in the Ni-I sample (Fig. 9).

310 Table 2 summarizes atomic ratios estimated from the EDX spectra of catalyst Ni-M and the  
311 regenerated sample of catalyst NiCo-M after their use in ESR test for 22h (and exposure to  
312 atmospheric air at room temperature). As shown, a huge amount of carbon is observed in both cases  
313 in agreement with TPO analysis, though a more moderate amount is detected in the case of Ni-M  
314 which agrees with the fact that this sample appears the most stable one among those examined in this  
315 work. This means that this type of carbon deposits does not impede catalytic activity, which is  
316 coherent with the nature of the carbon deposits observed by TEM. Interestingly, the surface atomic  
317 ratio of the used regenerated NiCo-M sample, Ni:Co = 3:2 suggests a surface enrichment in Ni, as  
318 compared with that of the fresh sample, Ni:Co=1.

### 319 3.5. General discussion

320 The most usual way to activate supported metal catalysts for steam reforming of alcohols is to reduce  
321 them in hydrogen to obtain the active metallic phase. However, pretreatment in pure hydrogen at  
322 relatively high temperature may cause metal sintering, decreasing the metal dispersion. The  
323 reduction by a softer reductant (as ethanol, for example; furthermore when combined with water in  
324 the ESR reactant mixture) may allow keeping metal dispersion closer to the initial one in the oxidic  
325 precursor. On the other hand, the activity of catalysts containing ceria is strongly dependent on the  
326 number of vacancies in its network, which in turn are dependent not only on the preparation method  
327 but also on its contact with the environment and its storage. For these reasons we used oxidative  
328 activation to homogenize the initial oxidation state of ceria in the catalysts, and let the reduction of  
329 the active metal component to take place by its interaction with the reaction medium. The positive  
330 effect of consecutive oxidation and reduction pretreatments has been reported in other supported

331 metallic systems: zeolite-supported nanosilver catalysts used for CO oxidation at low temperatures  
332 show much higher activity if they are pretreated consecutively first with oxygen and then reduced  
333 with hydrogen than if they are just only reduced in hydrogen at the same conditions [31]. XRD  
334 patterns evidenced that the base metal oxides phases present in the fresh samples are converted into  
335 metallic phases in all the used catalysts. Therefore, one may infer that both cations ( $\text{Ni}^{2+}$  and  $\text{Co}^{2+}$ )  
336 are reduced by the ethanol in the reactant mixture during the initial moments of their contact and  
337 then the ESR proceeds on the metallic centers generated. As our first product analysis is made after  
338 at least 15 minutes of the initial contact, the product distribution already corresponded to catalytic  
339 ESR and not to the initial stoichiometric redox reaction between the cations and ethanol.

340 The main effect of the preparation method was observed on the deactivation and the regenerability of  
341 the catalysts. Oxidative regenerations of the three impregnated catalysts recovered initial conversion  
342 values but the overall trend of catalyst deactivation, compared to that observed with the fresh  
343 samples, did not change, despite the initial different order of activity for the regenerated samples.  
344 The situation was quite different among the catalysts prepared by microemulsions. Monometallic  
345 Co-M showed deactivation trends similar to that of its impregnated homologous, Co-I, but its activity  
346 increased slightly after regeneration.

347 On the contrary, the catalytic performances, deactivation trends and effect of oxidative regeneration  
348 of the Ni-containing catalyst prepared by microemulsions (Ni-M, NiCo-M) was quite exceptional  
349 and totally different to their impregnated counterparts (Ni-I, NiCo-I).

350 Analysis of the distribution of the carbon-containing products and its evolution provides a key to  
351 understand the different behavior of the three catalysts prepared by microemulsions and the drastic  
352 change with the bimetallic catalyst. Besides  $\text{H}_2$ , the only products on the stable and most active  
353 catalyst, monometallic Ni-M, were  $\text{CO}_2$ , CO and  $\text{CH}_4$ , whose selectivity (55, 25 and 15%,  
354 respectively) did not vary along the run time, and traces of acetaldehyde. This suggests that the  
355 nickel active sites were very active in ethanol dehydrogenation to acetaldehyde (2), whose very little  
356 yield indicates it is rapidly transformed by steam reforming (4-5).

357 On the contrary, the main products on the fresh bimetallic NiCo-M were acetone and ethylene, which  
358 summed up 50 % of the carbon containing products. These two intermediates are known precursors  
359 of coke, which may have caused the quick deactivation; their absence among the products of Ni-M  
360 might explain its outstanding stability.

361 Acetone and ethylene were also formed in the initial test stages on fresh Co-M catalyst, but in lower  
362 proportion (the maximum joint yield was 32 %), and decreasing very fast until almost disappearing  
363 at 4 h on stream, a time after which the pace of deactivation slowed down. This similarity of their



364 product distribution seems to indicate that activity of the fresh NiCo-M catalysts is mostly  
365 determined by the Co atoms on its surface.

366 At a variance of the impregnated catalysts, the regeneration treatment of the two deactivated  
367 catalysts (both containing Co) improved their initial catalytic activity and their stability (Fig. 5,  
368 hollow symbols), overcoming their impregnated counterparts. The product distribution on reactivated  
369 Co-M catalyst was similar to the observed for the fresh sample, but formation of acetone and  
370 ethylene was much lower (combined selectivity 13 %), which may explain its smaller deactivation.

371 The most radical change caused by regeneration was observed with catalyst NiCo-M, which started  
372 to work almost like the most active Ni-M catalyst. Contrary to the first run of this sample, no  
373 formation of acetone and ethylene was observed on this regenerated sample; this fact (and the higher  
374 initial activity) would indicate a change in the chemical nature of its active sites, and an increase of  
375 their number, due to reactivation, thus resulting in a higher efficiency. The similarity of their product  
376 distribution to that of Ni-M catalyst seems to indicate that activity of the regenerated NiCo-M  
377 catalysts is mostly determined by the Ni atoms on its surface.

378 While in the impregnation the metal precursors are deposited onto the support surface, the reverse  
379 microemulsions method forms a precipitate in which the metal precursors can be mostly distributed  
380 in the bulk of the nanoparticles formed. The observed change in the NiCo-M behavior and the ESR  
381 product distribution after regeneration points to a change in its surface metal composition caused by  
382 the regeneration process. One may hypothesize that this could be due to an “emergence” of the active  
383 metal atoms from the bulk to the ceria nanoparticles surface. This can most likely be produced  
384 during the reduction of the system under the ESR mixture. Note a similar mechanism of metal  
385 surface segregation upon reduction of cations inserted in the ceria fluorite lattice was observed to  
386 occur in copper-doped ceria systems subjected to redox treatments [32]; as a difference with such  
387 case in which the bulk-surface migration of copper appeared basically reversible upon redox cycling  
388 [32], in our case the reoxidation during catalyst regeneration could apparently keep the metals at the  
389 sample surface with consequent increase in the activity. Indeed, the catalytic performance of this  
390 regenerated system is similar to that of Ni-M one. This is coherent with an emergence of Ni atoms in  
391 the regenerated NiCo-M, and the EDX analysis of this sample in fact suggests a surface enrichment  
392 of Ni, consistent with this hypothesis. Even so, the two samples have product distributions that  
393 suggest a difference in the nature of the active sites, as on the bimetallic NiCo-M acetaldehyde, the  
394 primary product in the reaction network, was never fully converted while on the catalyst Ni-M it is  
395 absent among the products, indicating its total transformation. This indicates that the active metal  
396 surface composition is not exactly the same, which is coherent with the slightly lower stability of  
397 regenerated NiCo-M.

398 Another point that may affect the evolution of the metals during reaction/regeneration is the presence  
399 of a big amount of coke present on the used sample after the ESR test. TPO profile shows that  
400 practically all the carbonaceous deposits on this sample are burned out below 650 °C. Even  
401 considering that the regeneration is made with a slow heating rate of 10 °C/min and with diluted  
402 oxygen, one may assume that such combustion can create very localized hot spots (or hot narrow  
403 regions) in the catalyst surface, where the much higher local temperature could alter the mobility of  
404 the atoms in the vicinity of the surface.

405

#### 406 **4. Conclusions**

407 The catalytic behavior in ESR of the (Ni, Co)-Ce-O system depends on the preparation method, the  
408 composition and its history. Freshly prepared catalysts are basically constituted by combinations of  
409 the cubic phases CeO<sub>2</sub>, NiO and Co<sub>3</sub>O<sub>4</sub>, but the latter are reduced to metallic Ni and Co during ESR  
410 reaction. All catalysts show high initial conversion but also deactivation, albeit at different rates,  
411 caused by carbonaceous deposits most likely formed from acetone and ethylene, which can be  
412 reversed by oxidation treatment with dilute O<sub>2</sub>.

413 The preparation methods investigated cause differences in the textural properties and crystallinity of  
414 the phases of the catalysts of the same composition, which influences their activity, stability, the type  
415 of the carbonaceous deposits formed during ESR and, therefore, their oxidative regenerability after  
416 their catalytic use. All this causes that the effect of the combination of Ni and Co in the bimetallic  
417 catalysts depends very much on its route of synthesis, producing a slight improvement, with respect  
418 to the monometallic Ni catalyst, only in the impregnated ones.

419 The reverse microemulsions method generates larger surface areas and a better dispersion of nickel,  
420 more homogeneous, which improves its activity and stability, as well as the yield and selectivity to  
421 H<sub>2</sub>. This made the Ni-CeO<sub>2</sub> (Ni:Ce = 4:6) catalyst prepared by this method (Ni-M) to be the most  
422 active one among those examined in this study. A significant improvement in performance and a  
423 change in the product distribution during the initial reaction stages is observed with the Co-  
424 containing catalysts prepared by microemulsion after oxidative regeneration, especially for the  
425 bimetallic NiCo-M catalyst, which points to a restructuring of the active centers during the reaction-  
426 regeneration cycle. We hypothesize that this could be due to the emergence of Ni atoms from the  
427 bulk to the ceria surface during reduction of the catalyst under ESR conditions and which can be  
428 affected by local overheating as a consequence of the burning of the carbon deposits during the  
429 oxidative regeneration treatment. Further characterization studies are in any case under way to verify  
430 this hypothesis.

431

432 **Aknowledgements**

433 This work was funded by MINECO projects CTQ2012-32928 and CTQ2015-71823-R. M. V. Vidal  
434 thanks to Departamento de Bolivar (Colombia) for her grant of the Grant Program "Bolivar Ganador".  
435 **Thanks are due to Unidad de Apoyo of ICP-CSIC for performing the characterization measurements.**

436

437 **References**

- 438 [1] S. Dutta, *J. Ind. Eng. Chem.* 20 (2014) 1148-1156.
- 439 [2] J.D. Holladay, J. Hu, D.L. King, Y. Wang. *Catal Today* 139 (2009) 244-260
- 440 [3] J. Llorca, V. Cortés Corberán, N. J. Divins, R. Olivera Fraile and E. Taboada, "Hydrogen from  
441 Bioethanol", in L. M. Gandia, G. Arzamendi, P. M. Dieguez (Eds.), "Renewable Hydrogen  
442 Technologies: Production, Purification, Storage, Applications and Safety", Elsevier Sci. & Technol.  
443 (2013), pp. 135-169., and references therein
- 444 [4] F. Rossillo-Calle, A. Walter. *Energy for Sustainable Development* 10 (2006) 20–32.
- 445 [5] S. I. Mussatto, G. Dragone, P. M.R. Guimarães, J. P. A. Silva, L. M. Carneiro, I. C. Roberto, A.  
446 Vicente, L. Domingues, J. A. Teixeira. *Biotechnol. Adv.* 28 (2010) 817–830
- 447 [6]. B. Bayram, I.I. Soykal, D. von Deak, J.T Miller, U.S. Ozkan. *J Catal* 284 (2011) 77-89.
- 448 [7] I. Llera, V. Mas, M. L. Bergamini, M. Laborde, N. Amadeo, *Chem Eng Sci* (2012) 356-66.
- 449 [8] A. Haryanto, S. Fernando, N. Muralli, S. Adhikari. *Energy Fuels* 19 (2005) 2089-106.
- 450 [9] R. M. Navarro, M. C. Sanchez-Sanchez, M. C. Alvarez-Galván, F. del Valle, J. L. G. Fierro.  
451 *Energy Environ. Sci.* 2 (2009) 35-54.
- 452 [10] L.V. Mattos, G. Jacobs, B.H. Davis, F.B. Noronha. *Chem. Rev.* 112 (2012) 4094-4123
- 453 [11] S. Li, J. Gong, *Chem. Soc. Rev.*, 43 (2014) 7245-7256.
- 454 [12] J. L. Contreras, J. Salmenes, J. A. Coli-Luna, L. Nuno, B. Quintana, I. Cordova, B. Zeifert, C.  
455 Tapia, G. A. Fuentes. *Int. J. Hydrogen Energy* 39 (2014), 18835-18853.
- 456 [13] T. Hou, S. Zhang, Y. Chen, D. Wang, W. Cai. *Renew. Sustain. Energy Rev.* 44 (2015) 132–148.
- 457 [14] D. Zanchet, J. B. O. Santos, S. Damyanova, J. M. R. Gallo, J. M. C. Bueno. *ACS Catal.* 5  
458 (2015) 3841-3863
- 459 [15] A. Kubacka, M. Fernandez-Garcia, A. Martinez-Arias. *Applied Catal.: A, General* 518 (2016)  
460 2-17
- 461 [16]. N. Laosiripojana, S. Assabumrungrat, S. Charojrochkul, *Applied Catal. A: General* 327 (2007),  
462 180–188
- 463 [17] V.A. de la Peña O’Shea, R. Nafria, P. Ramírez de la Piscina, N. Homs. *Int. J. Hydrogen Energy*  
464 33 (2008), 3601–3606.

- 465 [18] N. Homs, J. Llorca, P. Ramírez de la Piscina. *Catalysis Today* 116 (2006), 361–366
- 466 [19] G. Ozkana, S. Goka, G. Okan. *Chemical Engineering Journal* 171, (2011), 1270–1275.
- 467 [20] A. N. Fatsikostas, X. E. Verykios. *J. Catal.* 225 (2004), 439-452.
- 468 [21] J. Llorca, P. R. de la Piscina, J. Sales, N. Homs. *Chem. Comm.* 7 (2001), 641-642.
- 469 [22] S. Freni, S. Cavallaro, N. Mondello, L. Spadaro, F. Frusteri. *Catal. Comm.* 6 (2003), 259-268.
- 470 [23] A. Gutierrez, R. Karinen, S. Airaksinen, R. Kaila, A.O.I. Krause. *Int. J. Hydrogen Energy* 36
- 471 (2011) 8967-8977.
- 472 [24] A. M. Da Silva, K.R. de Souza, G. Jacobs, U.M. Graham, B.H. Davis, L.V. Mattos, F. B.
- 473 Noronha. *Applied Catal. B: Environmental* 102 (2011) 94-109.
- 474 [25] H. Song, U.S. Ozkan. *J. Catal.* 261 (2009), 66–74.
- 475 [26] D. Gamarra, G. Munuera, A. B. Hungría, M. Fernández-García, J. C. Conesa, P. A. Midgley, X.
- 476 Q. Wang, J. C. Hanson, J. A. Rodríguez, A. Martínez-Arias. *J. Phys. Chem. C* 111 (2007) 11026–
- 477 11038
- 478 [27] I. Carbajal, C.L. Bolívar-Díaz, A. Martínez-Arias, V. Cortés Corberán. *Actas SECAT 2015,*
- 479 *Barcelona (Spain), 13-15 July 2015, oral O3.2.*
- 480 [28] C.L. Bolívar-Díaz, I. Carbajal, A. Martínez-Arias, V. Cortés Corberán. *Actas SECAT 2015,*
- 481 *Barcelona (Spain), 13-15 July 2015, oral O8.2*
- 482 [29] A. Martínez-Arias, M. Fernández-García, V. Ballesteros, L. N. Salamanca, J. C. Conesa, C.
- 483 Otero, J. Soria. *Langmuir* 15 (1999) 4796.
- 484 [30] Lj. Kundakovic and M. Flytzani-Stephanopoulos. *J. Catal.* 179 (1998) 203-221
- 485 [31] E. Kolobova, A. Pestryakov, G. Mamontov, Yu. Kotolevich, N. Bogdanchikova, M. Farias, A.
- 486 Vosmerikov, L. Vosmerikova, V. Cortés Corberán. *Fuel* 188 (2017) 121-131.
- 487 [32] X. Wang, J.A. Rodriguez, J.C. Hanson, D. Gamarra, A. Martínez-Arias, M. Fernández-García.
- 488 *J. Phys. Chem. B* 109 (2005) 19595-19603.

489

490 **Table 1:** Textural and phase characterization of as-prepared catalysts

Catalyst	BET		XRD	
	Surface area (m <sup>2</sup> /g)	Average pore diameter (nm)	Lattice parameter <i>a</i> (nm)	Crystal size (nm)
Ni- <i>I</i>	76	4.0	0.5411	8.0
NiCo- <i>I</i>	72	5.7	0.5389	7.5
Co- <i>I</i>	70	4.2	0.5411	7.8
Ni- <i>M</i>	136	4.0	0.5454	3.7
NiCo- <i>M</i>	132	4.2	0.5330	3.9
Co- <i>M</i>	125	5.2	0.5482	4.2

491

492 **Table 2:** EDX analysis of Ni-M and regenerated NiCo-M catalysts after their use in ESR

493

Catalyst	EDX atomic composition (at. %)				
	C	O	Ni	Co	Ce
Ni-M	93.34	3.68	0.84	-	1.11
NiCo-M	99.51	1.36	0.29	0.19	0.02

494

495

496 **Legend of the figures**

497 Fig. 1. XRD patterns of the CeO<sub>2</sub> support (orange) and the impregnated catalysts: Ni-I (blue), NiCo-I  
498 (green), Co-I (red)

499 Fig. 2: XRD patterns of the catalysts prepared by reverse microemulsions method: Ni-M (blue),  
500 NiCo-M (green), Co-M (red).

501 Fig. 3. Ethanol steam reforming on fresh impregnated catalysts at 500°C: ethanol conversion (left)  
502 and hydrogen yield (right) as function of reaction time.

503 Fig. 4. Ethanol steam reforming on used impregnated catalysts (*I*) after reactivation: ethanol  
504 conversion as function of reaction time. Reaction conditions in text.

505 Fig. 5. Ethanol steam reforming on fresh (solid symbols) and reactivated (hollow symbols) catalysts  
506 prepared by reverse microemulsions (M): ethanol conversion (left) and hydrogen yield (right) as  
507 function of reaction time. Reaction conditions in text.

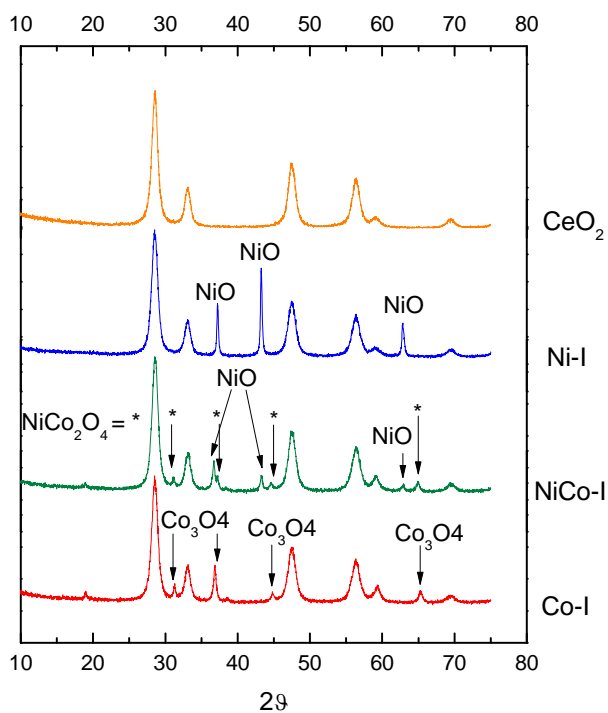
508 Fig. 6. XRD patterns of the used samples of catalysts of Ni (blue) NiCo (green) and Co (red)  
509 prepared by impregnation (I, top) and reverse microemulsions method (M, bottom). Sharp peaks at  
510  $2\theta = 35^\circ$  correspond to sample contamination with SiC, used as catalytic bed diluent during the tests.

511 Fig. 7. CO<sub>2</sub> formation profiles during TPO of the used samples of catalysts of Ni (blue) NiCo (green)  
512 and Co (red) prepared by impregnation (I, top) and reverse microemulsions method (M, bottom).

513 Fig 8. TEM images of fresh (left) and used (right) samples of impregnated Ni-I catalyst.

514 Fig 8. TEM images of the used sample of impregnated Ni-M catalyst.

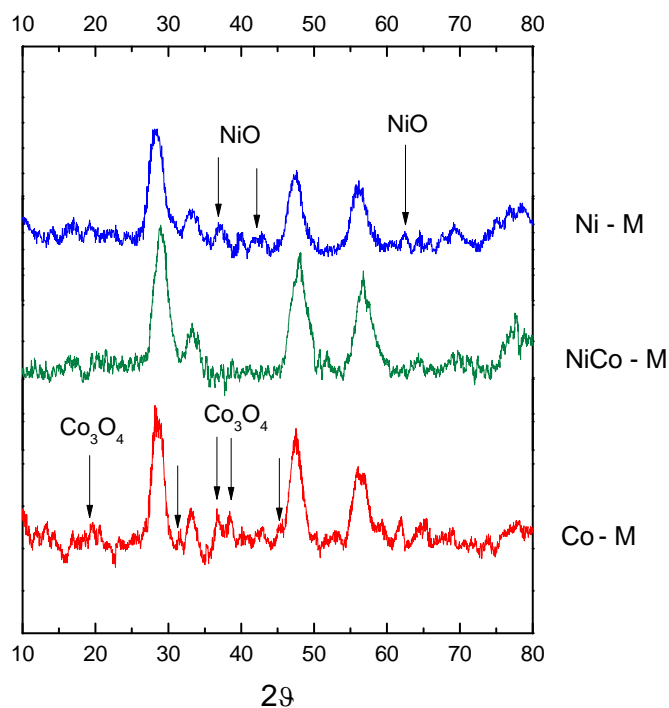
515



516

517 **Fig. 1:** XRD patterns of the CeO<sub>2</sub> support (orange) and the impregnated catalysts: Ni-I (blue), NiCo-I  
518 (green), Co-I (red)

519

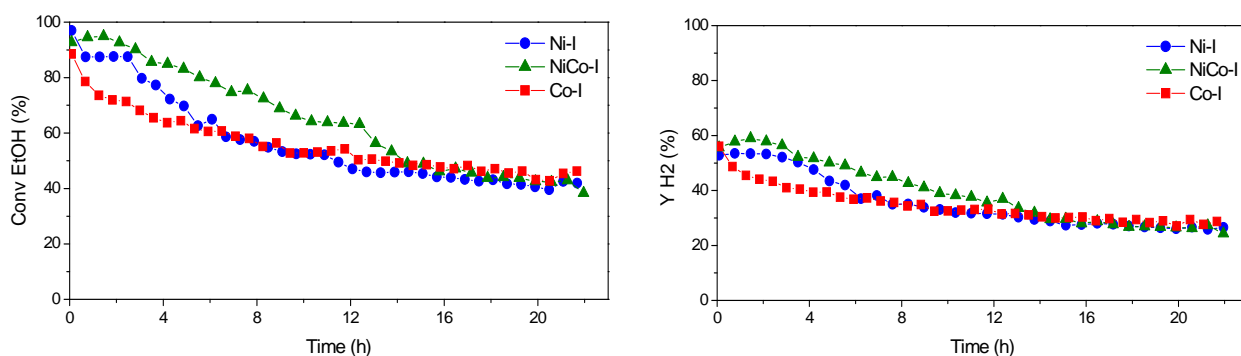


520

521 **Fig. 2:** XRD patterns of the catalysts prepared by reverse microemulsions method: Ni-M (blue),  
522 NiCo-M (green), Co-M (red).

523

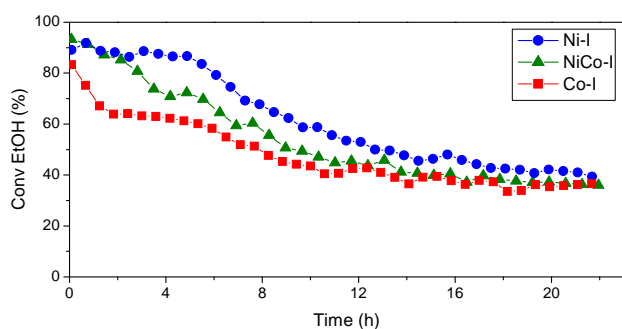
524



525

526 **Fig 3:** Ethanol steam reforming on fresh impregnated catalysts (*I*): ethanol conversion (left) and  
527 hydrogen yield (right) as function of reaction time. Reaction conditions in text.

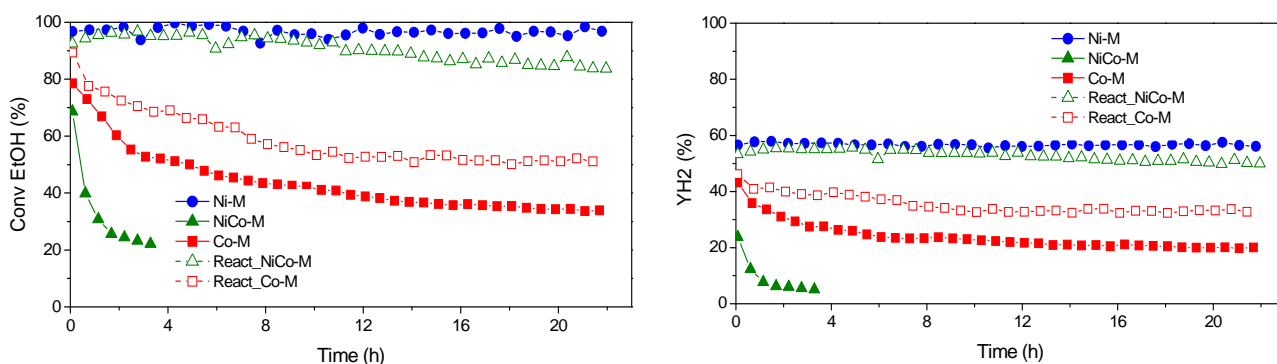
528



529

530 **Fig 4:** Ethanol steam reforming on used impregnated catalysts (*I*) after reactivation: ethanol  
531 conversion as function of reaction time. Reaction conditions in text.

532



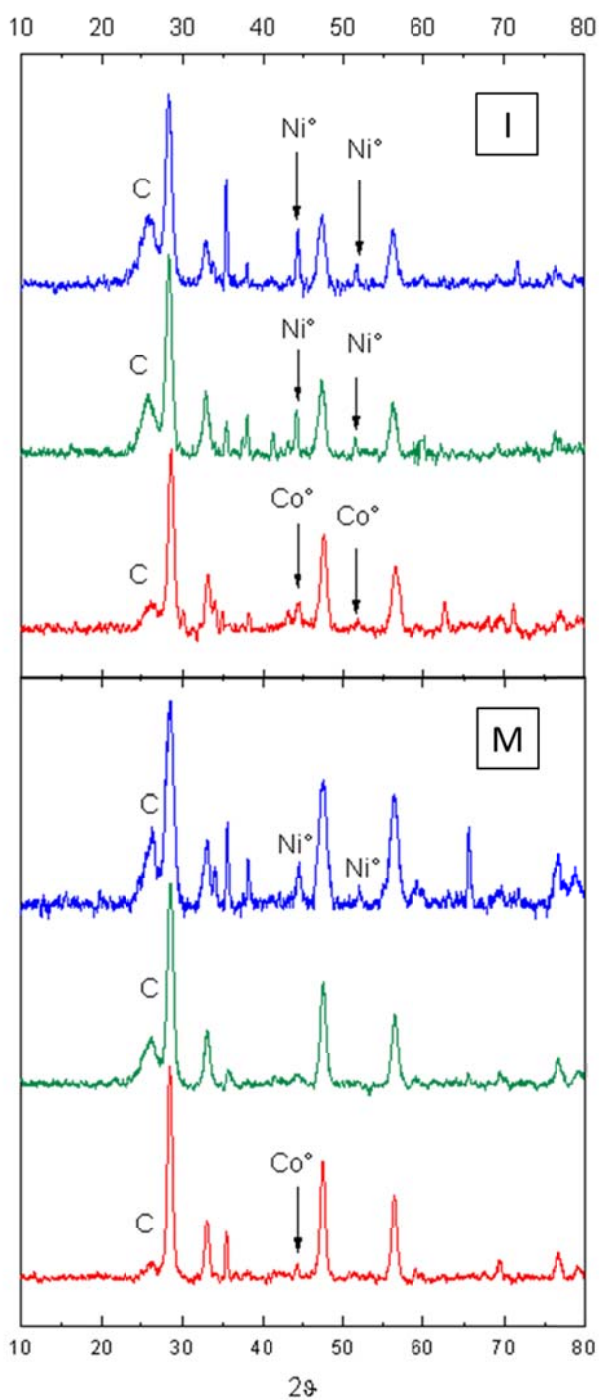
533

534 **Fig 5:** Ethanol steam reforming on fresh (solid symbols) and reactivated (hollow symbols) catalysts  
535 prepared by reverse microemulsions (*M*): ethanol conversion (left) and hydrogen yield (right) as  
536 function of reaction time. Reaction conditions in text.

537

538





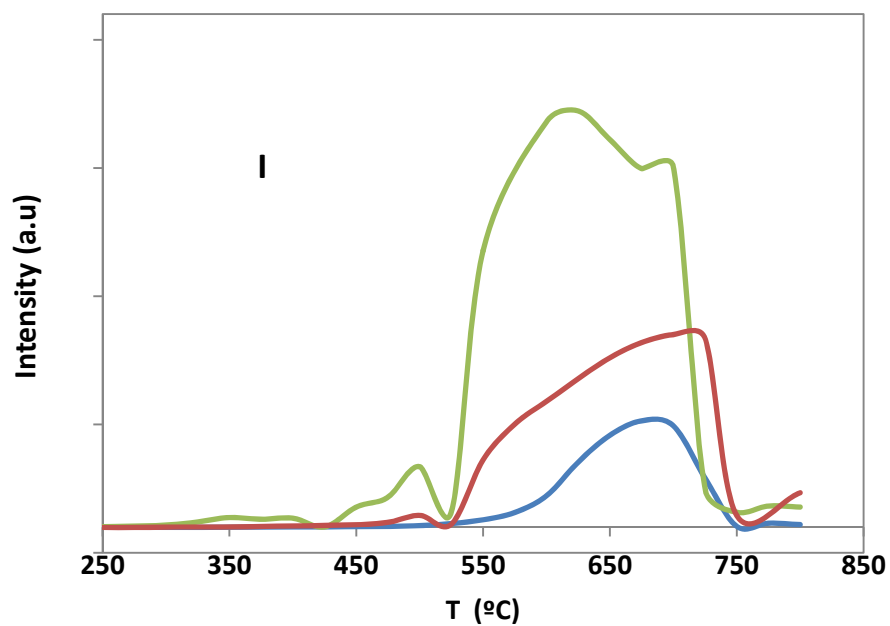
540

541 **Fig. 6:** XRD patterns of the used samples of catalysts of Ni (blue) NiCo (green) and Co (red)  
 542 prepared by impregnation (I, top) and reverse microemulsions method (M, bottom). Sharp peaks at  
 543  $2\theta = 35^\circ$  correspond to sample contamination with SiC, used as catalytic bed diluent during the tests.

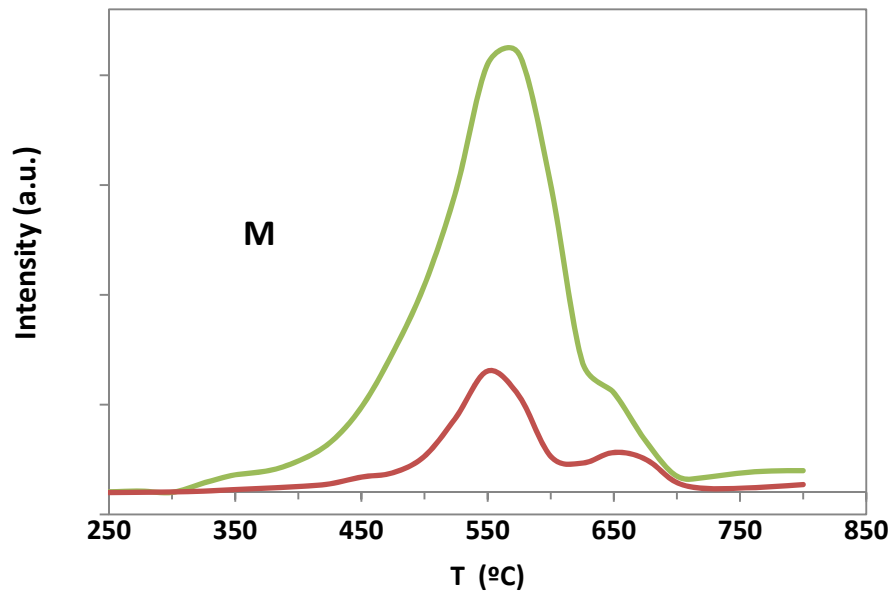
544

545

546



547



548

549

550

551 Fig. 7. CO<sub>2</sub> formation profiles during TPO of the used samples of catalysts of Ni (blue) NiCo (green)

552 and Co (red) prepared by impregnation (I, top) and reverse microemulsions method (M, bottom).

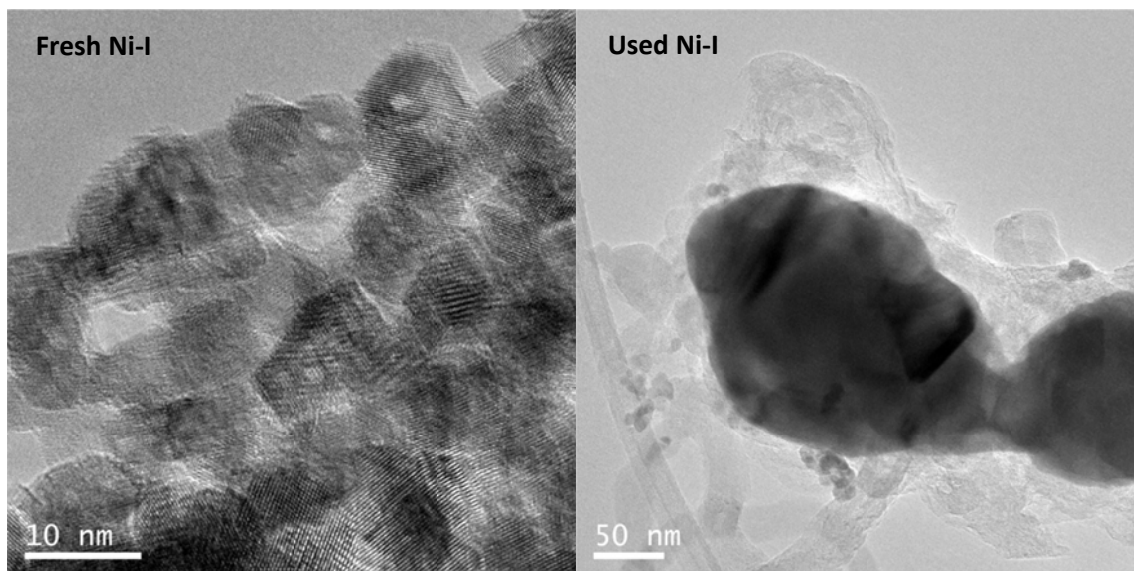
553

554

555

556

557



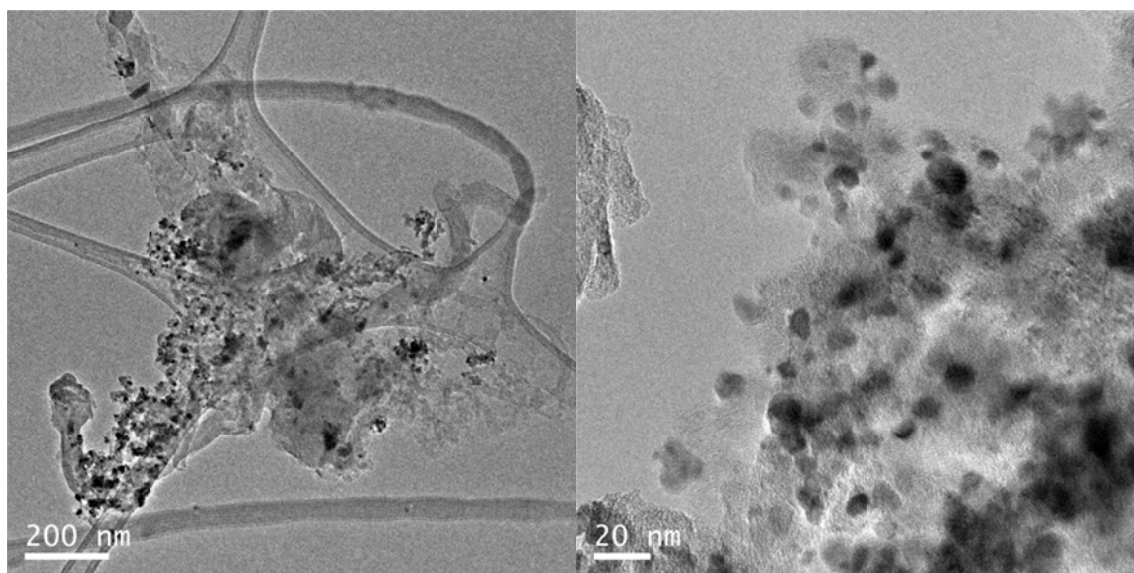
558

559

560 Fig 8. TEM images of fresh (left) and used (right) samples of impregnated Ni-I catalyst.

561

562



563

564

565 Fig 8. TEM images of the used sample of Ni-M catalyst from microemulsions